Earth and Planetary Science Letters 275 (2008) 54–60

Contents lists available at ScienceDirect

Earth and Planetary Science Letters

journal homepage: www.elsevier.com/locate/epsl

Fossil dripwater in stalagmites reveals Holocene temperature and rainfall variation in Amazonia

M.R. van Breukelen [a,b], H.B. Vonhof [a,*], J.C. Hellstrom [c], W.C.G. Wester [a], D. Kroon [a,d]

[a] Faculty of Earth and Life Sciences, Vrije Universiteit Amsterdam, De Boelelaan 1085, 1081HV, Amsterdam, The Netherlands
[b] Present address: Netherlands Forensic Institute, Laan van Ypenburg 6, 2497 GB, The Hague, The Netherlands
[c] School of Earth Sciences, University of Melbourne, Parkville, VIC, 3010 Australia
[d] Present address: School of Geosciences, West Mains Road, EJ9 3JW, Edinburgh, Scotland

ARTICLE INFO

Article history:
Received 21 May 2008
Received in revised form 30 July 2008
Accepted 31 July 2008
Available online 20 September 2008

Editor: P. DeMenocal

Keywords:
speleothem
fluid inclusions
stable isotope
South America

ABSTRACT

Most proxy records used for reconstruction of Holocene climate of Amazonia are unable to quantitatively distinguish between the effect of temperature and rainfall amounts.
We present a new isotope technique applied to a ~13,500 yr stalagmite archive from Peruvian Amazonia. By analysing the coupled isotope composition of fossil dripwater trapped in stalagmite fluid inclusions, and that of the calcite hosting the fluid inclusions, we were able to calculate independent paleotemperatures and rainfall amounts.
This stalagmite record shows that Holocene climate variation was controlled by orbitally-forced Southward migration of the Inter Tropical Convergence Zone. While temperature remained constant, isotope variation of rainwater, reflected in fluid inclusion water $\delta^{18}O$ composition, suggests a ~15–30% increase in convective rainfall through the Holocene.
A comparison of the low-land Peruvian fluid inclusion record with the high Andean Huascaran ice core record shows a constant ~12‰ offset of $\delta^{18}O$ curves for the Holocene, suggesting that Andean vertical temperature gradients (lapse rates) did not vary much over the last 9000 years. During the Younger Dryas interval, however, the offset of $\delta^{18}O$ values was much higher than in the Holocene. This may be attributed to a relative drop in air temperatures in the highlands (higher lapse rate), caused by long distance teleconnections to climate perturbations in the North Atlantic.
In a wider perspective, fluid inclusion isotope analysis drastically improves paleotemperature reconstructions based on speleothem calcite $\delta^{18}O$ data, because it provides the $\delta^{18}O$ value of drip water through time, which is usually the most important unknown in paleotemperature equations.

1. Introduction

The climate history of the Amazon Basin has been studied intensively over the last decades, with particular focus on Glacial-Interglacial variability, and its effect on biodiversity in Amazonia (Hooghiemstra and van der Hammen, 1998). Of crucial importance for our understanding of the relation between climate and biodiversity is our ability to quantitatively determine temperature and rainfall variation in space and time. However, nearly all currently applied climate proxy records in Amazonia are affected by temperature as well as rainfall amounts (Hooghiemstra and van der Hammen, 1998; Thompson et al., 2000). This is particularly limiting for the interpretation of high-resolution stable isotope climate records, like ice cores (Thompson et al., 1995, 2000; Ramirez et al., 2003), lacustrine calcite (Seltzer et al., 2000) and speleothems (Cruz et al., 2005). While these isotope records are highly valuable for our understanding of high resolution Holocene climate variation, quantification of the variation of temperature relative to rainfall amounts remains problematic.

Here, we present new speleothem-based isotope records from Peruvian Amazonia, which allow quantification of the effect of temperature and rainfall amounts on isotope signals in Amazonia. Of pivotal importance in the present study is the application of a technique to analyze the stable isotope composition of fossil dripwater trapped as fluid inclusions in speleothem calcite (Vonhof et al., 2006, 2007).

Speleothems (stalagmites) commonly contain microscopic water-filled cavities. These so-called fluid inclusions are filled with cave drip water from the time of formation of the relevant speleothem growth increment (Schwarcz et al., 1976; Harmon et al., 1979). It has been established that cave drip water, and thus fluid inclusion water, is isotopically identical to local rainwater (for $\delta^{2}H$ and $\delta^{18}O$; Caballero et al., 1996; McDermott et al., 2006). In arid regions cave drip water may deviate from rainwater due to evaporation. However, this is not likely to be the case in the humid tropical climate of our study area.

* Corresponding author.
E-mail address: hubert.vonhof@falw.vu.nl (H.B. Vonhof).

0012-821X/$ – see front matter © 2008 Elsevier B.V. All rights reserved.
doi:10.1016/j.epsl.2008.07.060

Speleothem calcite hosting the fluid inclusions can be dated at high precision by Uranium-series chronology (Richards and Dorale, 2003; McDermott et al., 2006).

Stable isotope records from speleothem calcite are commonly used as paleoclimate proxy (Bar-Matthews et al., 1999; Wang et al., 2001; Fleitmann et al., 2003; Genty et al., 2003; Yuan et al., 2004; Cruz et al., 2005; Wang et al., 2005). It is a powerful tool, because a wide variety of climate phenomena like El Niño events (Frappier et al., 2002), the Little Ice Age (Holmgren et al., 1999), the Younger Dryas (Bar-Matthews et al., 1999; Yuan et al., 2004; Vacco et al., 2005; Genty et al., 2006) and Dansgaard Oeschger events (Wang et al., 2001; Genty et al., 2003) are recognised in these isotope records. Oxygen isotope records of carbonates are commonly used as a direct paleotemperature proxy, because at known $\delta^{18}O$ values of formation water and calcite that forms from it, the temperature of calcite formation can be calculated (Epstein et al., 1953; Craig, 1965; Kim and O'Neil, 1997). This proxy system is based on the known temperature dependency of oxygen isotope fractionation between calcite and the water in which the calcite precipitates. The most important limitation for the application of this proxy to calculate paleotemperatures concerns the uncertainty on the assumed $\delta^{18}O$ value of past formation water. For marine records, this is not too much of a problem because past $\delta^{18}O$ variation in the oceans is limited, and relatively well understood (Shackleton and Opdyke, 1973). However, for continental records like speleothems, climate change affects drip water isotope composition in a less predictable way. Therefore, quantification of the contribution of temperature to speleothem $\delta^{18}O$ records is impossible based on the $\delta^{18}O$ value of the speleothem calcite alone (Hendy and Wilson, 1968; Harmon et al., 1978; Schwarcz and Yonge, 1983; Fairchild et al., 2006).

The ability to analyse stalagmite fluid inclusion $\delta^{18}O$ values eliminates the uncertainty associated with reconstruction of drip water $\delta^{18}O$ values back in time, and thus allows for the reconstruction of independent speleothem growth temperatures based on paired fluid inclusion and host $CaCO_3$ $\delta^{18}O$ values. Since drip water isotope composition is believed to reflect that of rainfall recharging the cave aquifer, fluid inclusion isotope values in stalagmites furthermore provide temporal records of rainfall isotope variation which can be related to changing rainfall patterns through time (McDermott et al., 2006; Vonhof et al., 2006).

2. Results

We analysed $\delta^{18}O$ values of fluid inclusions and host calcite of speleothems collected in the Cueva del Tigre Perdido near the town of Nueva Cajamarca in the Peruvian district San Martín (Fig. 1). This cave lies in a densely vegetated area in the foothills of the Andes, at ~1000 meter above sealevel. The composite record consists of two stalagmites, with an age model based on 15 TIMS U-series ages from the lab of VU University Amsterdam, and 5 additional MC-ICP-MS ages from the lab of Melbourne University (Fig. 2, Table 1; see also the additional material). A high-resolution $\delta^{18}O$ record of speleothem calcite shows a long cycle through the Holocene (Fig. 3), with an amplitude of ~2‰.

Petrographic analysis of both speleothems studied, reveals the presence of abundant fluid inclusions in speleothem calcite (Fig. 4). Speleothem mineralogy and fluid inclusions are interpreted to be primary, which leads us to conclude that fluid inclusion isotope composition is undisturbed since the time of formation.

A total of 18 cubes of speleothem calcite, weighing ~0.3 g each, were cut from a central slab of the stalagmites, crushed, and the liberated inclusion water analyzed for $\delta^{2}H$ and $\delta^{18}O$, applying the technique described by Vonhof et al. (2006, 2007).

Results show ~15‰ variation in $\delta^{2}H$ values and ~2‰ in $\delta^{18}O$ values. $\delta^{2}H$ values of the youngest part of the stalagmite record plot at approximately −42‰ (SMOW) which is in reasonably good agreement with the −46‰ value analysed for some local rain-showers and from the river that runs through the cave. $\delta^{18}O$ and $\delta^{2}H$ values combined plot on the Global Meteoric Water Line (GMWL; Fig. 5). Since modern rainwater isotope data for Amazonia generally plot on the GMWL (Gat and Matsui, 1991), this observation provides further support for the excellent preservation of the original isotope composition of fluid inclusion water in these speleothems, P post-depositional changes in the fluid inclusion water isotope composition would have driven the water away from the GMWL. Three cubes, however, gave isotope values that plotted away from the GMWL. These were samples with a low water yield (<0.1 µl), resulting in erroneous $\delta^{18}O$ values, as was confirmed by

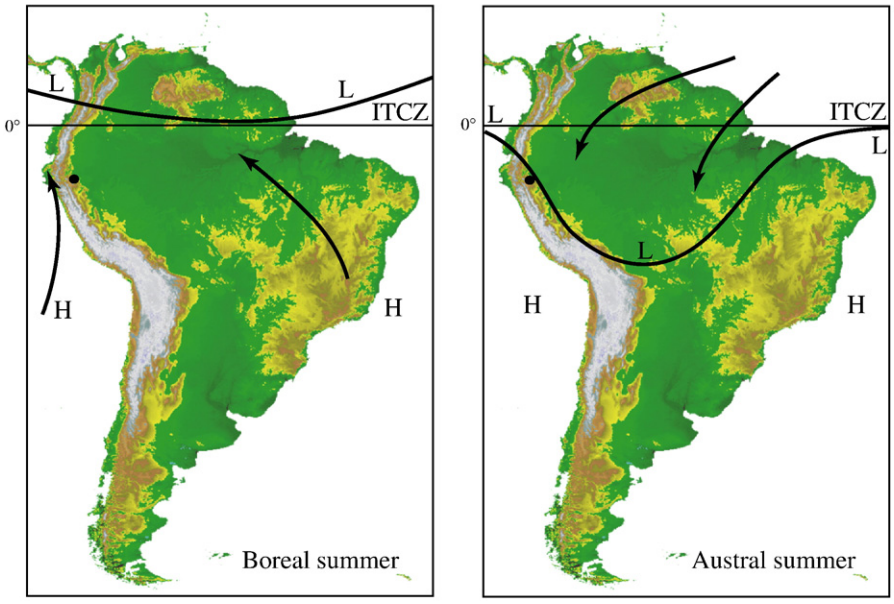

Fig. 1. Map of South America showing the generalized position of the Inter Tropical Convergence Zone (ITCZ; black line) during Boreal summer (July) and Austral summer (January). The black dot marks the position of Cueva del Tigre Perdido, which lies under the ITCZ in Austral summer. Arrows indicate the prevailing wind direction, during the season. "H"and "L indicate the position of high- and low pressure areas.

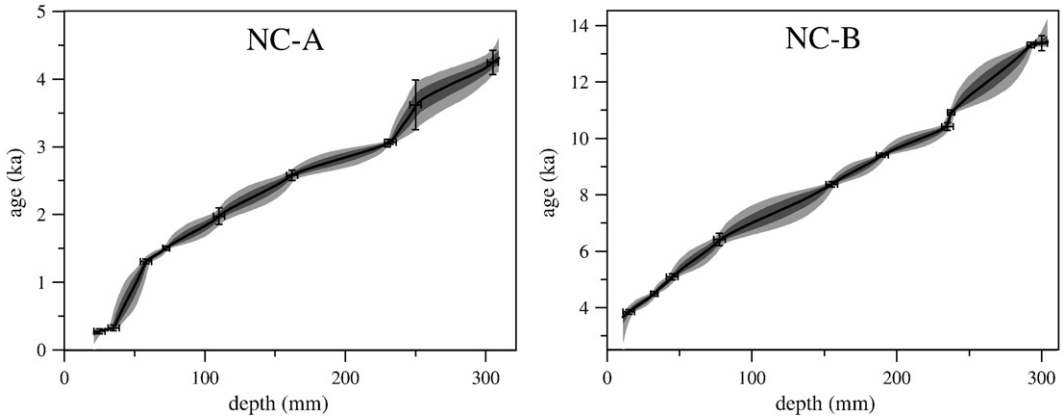

Fig. 2. Age model of stalagmites NC-A and NC-B. Shown are all TIMS and ICP-MS uranium series ages from labs in Amsterdam and Melbourne combined. 1 and 2 sigma errors are indicated in different shades. Procedure for U and Th isotope analysis at the VU University Amsterdam is given in the additional materials. Procedure for U and Th isotope analysis at the University of Melbourne is described in detail in Hellstrom (2003). The age correction is according to equation 1 of Hellstrom (2006), for an initial [230/232] of 1.5 ± 1.5. The age-depth modelling techniques used are as described in the supplementary materials of Drysdale et al. (2005).

yield tests with an in-house water standard. Duplication of two of these analyses with larger cubes of calcite, suggests that the δ^2H values of these low-yield samples are accurate, but the δ^{18}O values are not. For the following discussion of the data, only the δ^{18}O values of these three low-yield samples were discarded.

3. Discussion

Results are plotted stratigraphically in Fig. 3. The δ^2H and δ^{18}O values of fluid inclusion water appear to vary in phase with speleothem calcite δ^{18}O values and with orbitally-forced wet season (February) insolation (Fig. 3). After an isotope maximum at ~9000 years BP, coincident with the Holocene insolation minimum, a trend towards lower isotope values runs parallel with slowly increasing insolation energy.

Such a Holocene isotope pattern is not unique in Amazonia. Similar isotope trends were reported for the Andean Ice cores (Thompson et al., 2000, 2006) and Lake Junin on the Peruvian Altiplano (Seltzer et al., 2000) (Fig. 6). Although small differences exist, the general Holocene trend for all these records appears to be insolation-forced.

Although the patterns are similar, the interpretation of these records in terms of Holocene temperature and rainfall variation is still debated. Some interpret the Holocene isotope pattern to be mainly temperature controlled (Thompson et al., 1995, 2000), while others advocate rainfall as the controlling parameter (Broecker, 1997; Henderson et al., 1999; Seltzer et al., 2000; Ramirez et al., 2003; Vimeux et al., 2005).

Insolation forcing of Holocene Amazonian climate may have affected temperature as well as rainfall amounts, because increased insolation energy can raise surface temperatures, or convert to latent heat and enhance convective rainfall (Thompson et al., 2000; Vuille et al., 2003).

In our study area in Northern Peru, insolation controls the dynamics of the Inter Tropical Convergence Zone (ITCZ; Fig. 1). This results in characteristic seasonal rainfall patterns as the ITCZ band of maximum convection migrates over the continent tracking the latitudinal displacement of maximum insolation (Marengo and Nobre, 2001). An orbitally-forced southward displacement of the complete ITCZ system through the Holocene resulted in a gradual increase in convective rainfall in our study area, as opposed to a decrease of rainfall over northern South America (Seltzer et al., 2000; Haug et al., 2001). Intensification of convective rainfall typically decreases δ^{18}O values of rain water (Garreaud et al., 2003; Vuille et al., 2003). Southward displacement of the ITCZ system in the Holocene and the associated increase of total insolation in our study area may also have had an effect on surface temperatures, if one assumes that part of the increase in insolation energy was not converted to latent heat (Rozanksi and Araguás-Araguás, 1995).

Table 1
All U–Th ages from Amsterdam and Melbourne labs combined

Sample	Depth (mm)	2s	[230/238]	2s	[234/238]	2s	Age(suppl.) (ka)	2s	[232/238]	2s	AgeCorr [0/2]i = 1.5 ± 1.5	2s	[234/238]i corr	2s	
NC-A	25.0	4.0	0.0045	0.0003	1.5986	0.0019	0.306	0.022	0.000288	0.000021	0.277	0.036	1.5991	0.0019	Amsterdam
NC-A	35.0	4.0	0.0049	0.0006	1.5997	0.0256	0.337	0.047	0.000076	0.000009	0.326	0.043	1.6002	0.0260	Amsterdam
NC-A	58.0	4.0	0.0191	0.0005	1.5960	0.0014	1.313	0.037	0.000020	0.000001	1.306	0.035	1.5982	0.0014	Amsterdam
NC-A	72.5	2.5	0.0217	0.0004	1.5603	0.0035	1.524	0.031	0.000153	0.000001	1.506	0.033	1.5626	0.0034	Melbourne
NC-A	110.0	4.0	0.0302	0.0008	1.5927	0.0014	2.089	0.055	0.001051	0.000034	1.975	0.123	1.5960	0.0014	Amsterdam
NC-A	162.0	4.0	0.0384	0.0002	1.5874	0.0013	2.674	0.013	0.000758	0.000015	2.581	0.078	1.5917	0.0013	Amsterdam
NC-A	230.0	2.0	0.0440	0.0007	1.5715	0.0028	3.087	0.051	0.000272	0.000002	3.057	0.057	1.5765	0.0028	Melbourne
NC-A	232.0	4.0	0.0449	0.0004	1.6044	0.0012	3.092	0.031	0.000147	0.000003	3.067	0.031	1.6097	0.0012	Amsterdam
NC-A	250.0	4.0	0.0578	0.0009	1.6079	0.0014	3.989	0.067	0.003516	0.000089	3.618	0.367	1.6142	0.0016	Amsterdam
NC-A	305.0	4.0	0.0630	0.0003	1.5759	0.0014	4.447	0.025	0.001709	0.000035	4.247	0.178	1.5829	0.0014	Amsterdam
NC-B	15.0	4.0	0.0542	0.0011	1.5500	0.0009	3.883	0.085	0.000142	0.000004	3.850	0.081	1.5560	0.0009	Amsterdam
NC-B	32.5	2.5	0.0623	0.0008	1.5193	0.0030	4.547	0.060	0.000477	0.000003	4.493	0.080	1.5259	0.0031	Melbourne
NC-B	45.0	4.0	0.0733	0.0007	1.5714	0.0009	5.200	0.057	0.000871	0.000019	5.091	0.104	1.5797	0.0009	Amsterdam
NC-B	77.5	4.0	0.0916	0.0028	1.5763	0.0011	6.517	0.211	0.000696	0.000026	6.419	0.222	1.5869	0.0012	Amsterdam
NC-B	155.0	4.0	0.1194	0.0003	1.5876	0.0008	8.498	0.029	0.000922	0.000019	8.371	0.097	1.6017	0.0008	Amsterdam
NC-B	190.0	4.0	0.1346	0.0009	1.6150	0.0007	9.454	0.071	0.000059	0.000001	9.409	0.065	1.6316	0.0007	Amsterdam
NC-B	235.0	4.0	0.1482	0.0019	1.6115	0.0008	10.473	0.143	0.000144	0.000003	10.418	0.141	1.6298	0.0009	Amsterdam
NC-B	237.5	2.5	0.1514	0.0011	1.5740	0.0027	10.931	0.082	0.000132	0.000001	10.922	0.086	1.5921	0.0027	Melbourne
NC-B	292.5	2.5	0.1793	0.0011	1.5433	0.0029	13.340	0.085	0.000291	0.000002	13.308	0.095	1.5641	0.0030	Melbourne
NC-B	300.0	4.0	0.1832	0.0034	1.5725	0.0009	13.427	0.270	0.000048	0.000001	13.376	0.262	1.5946	0.0010	Amsterdam

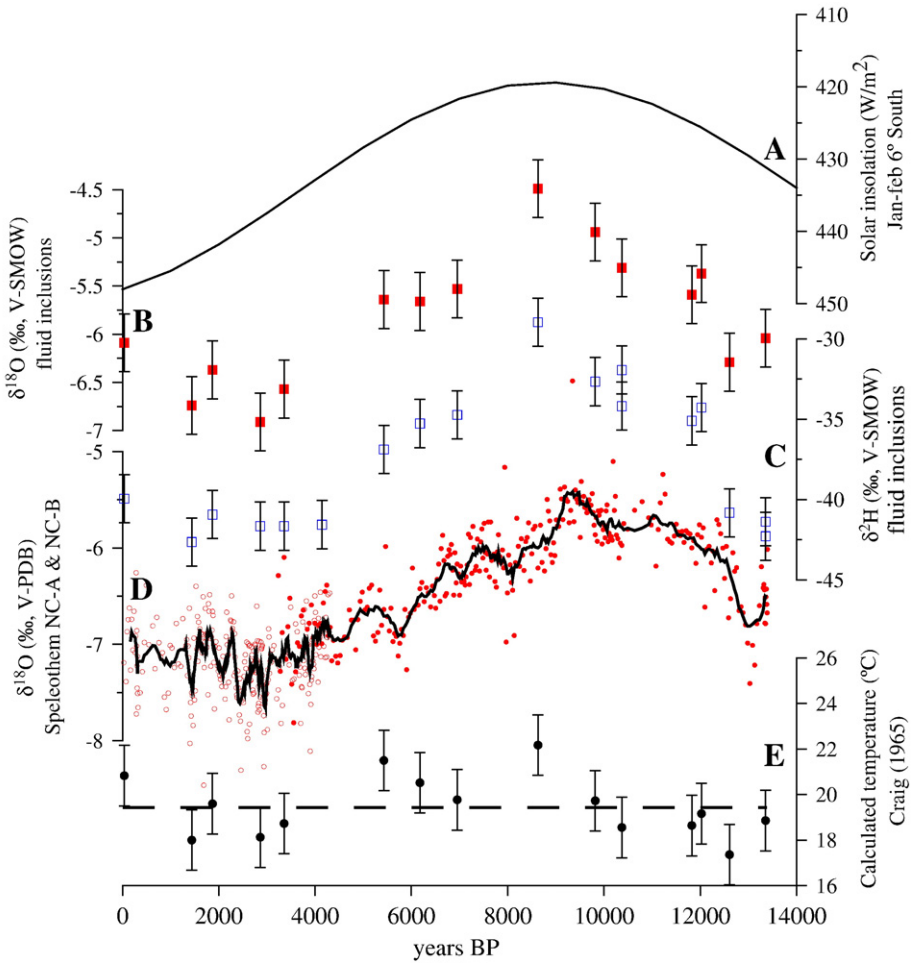

Fig. 3. Plot of the February solar insolation curve at 6° South (Laskar et al., 2004) (panel A) compared with isotope data obtained from the Cueva del Tigre Perdido record. Shown are $\delta^{18}O$ values (panel B) and $\delta^{2}H$ values (panel C) of fluid inclusion water. Dating error is smaller then the size of the symbol used. Panel D shows $\delta^{18}O$ values of speleothem calcite. Long term trends in all isotope records are in phase with the solar insolation curve. Paleotemperatures, shown in panel E, are calculated based on $\delta^{18}O$ data from panel B and D, using the paleotemperature equation by Craig (1965). Horizontal dashed line in panel E represents the average temperature calculated. Error bars on fluid inclusion isotope data and on calculated temperatures are based on 1SD reproducibility of standard waters routinely analyzed within fluid inclusion isotope runs (Vonhof et al., 2007). In panel D, solid (open) dots represent data from the NC-B (NC-A) stalagmite. The black solid curve represents an 11-point running average through the data.

The Tigre Perdido stalagmite record offers new insights in the relative changes of temperature and convective rainfall through the Holocene, because this record provides independent paleotemperatures and rainfall isotope composition. Paleotemperatures are calculated by using coupled calcite $\delta^{18}O$ and fluid inclusion $\delta^{18}O$ values as input parameters in a paleotemperature equation. Most commonly used for inorganically precipitated calcite is the equation by Kim and O'Neil (1997). Resulting paleotemperatures for the Tigre Perdido

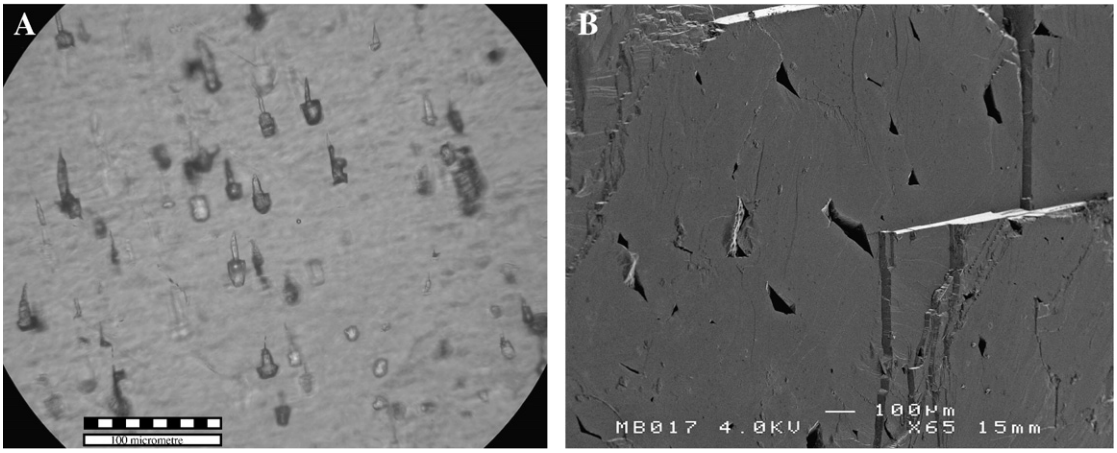

Fig. 4. Petrographic images of typical fluid inclusions found in the stalagmites studied. A) provides an example of fluid inclusions patterns in thin sections of NC-B stalagmite. B) Scanning Electron Microscope (SEM) image of a freshly broken calcite surface from NC-B, showing dense calcite with relatively large fluid inclusions. Distribution and geometry of fluid inclusions suggest that they are not interconnected and have not been diagenetically modified since their formation.

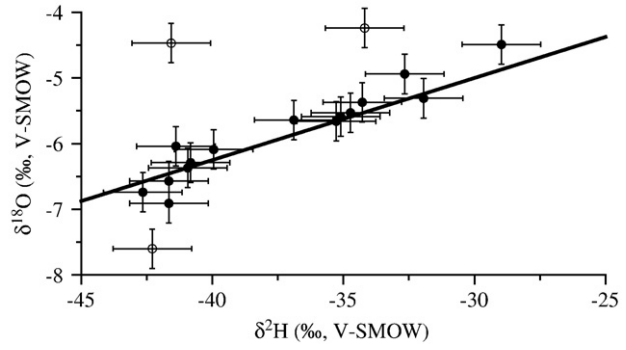

Fig. 5. $\delta^{18}O$ and $\delta^{2}H$ values of all analysed fluid inclusion samples. The black line represents the Global Meteoric Water Line (GMWL) Most fluid inclusion values plot on the GMWL, except for three obvious outliers (open dots). These three samples had the lowest water yields of the dataset at <0.1 μL per crush. Standard water injection experiments confirmed that $\delta^{18}O$ values are no longer reproducible at such low water yields, leading us to reject the $\delta^{18}O$ values of these three low-yield samples. Subsequent duplicate analysis of two of these three samples confirmed that $\delta^{2}H$ values of the low-yield samples were still reliable.

record show little variation, as to be expected for this area in the Holocene. However, at ~17 °C, calculated temperatures are much lower than the modern cave temperature which lies at ~22 °C. This apparent mismatch is a well known phenomenon for speleothem based paleotemperature reconstructions. Mickler et al. (2004) show that modern speleothem calcite from Barbados precipitates in oxygen isotope disequilibrium, and suggest that this is due to kinetic fractionation. Such fractionation will lead to calculated paleotemperatures that can be several °C too low. A recent compilation of available cave monitoring data, McDermott et al. (2006) demonstrates that this effect occurs in other caves as well. This compilation further shows that among the different paleotemperature equations available, the Kim and O'Neil (1997) equation leads to temperatures that are several °C too low. More accurate temperatures appear to be calculated by the equation of Craig (1965). Application of the Craig (1965) equation to the Tigre Perdido record results in a Holocene paleotemperature of ~20 °C (Fig. 3), indeed much closer to modern cave temperatures of ~22 °C than the 17 °C calculated from the Kim and O'Neil (1997) equation. The total observed variation around the mean value does not exceed the analytical uncertainty on the input parameters, which are

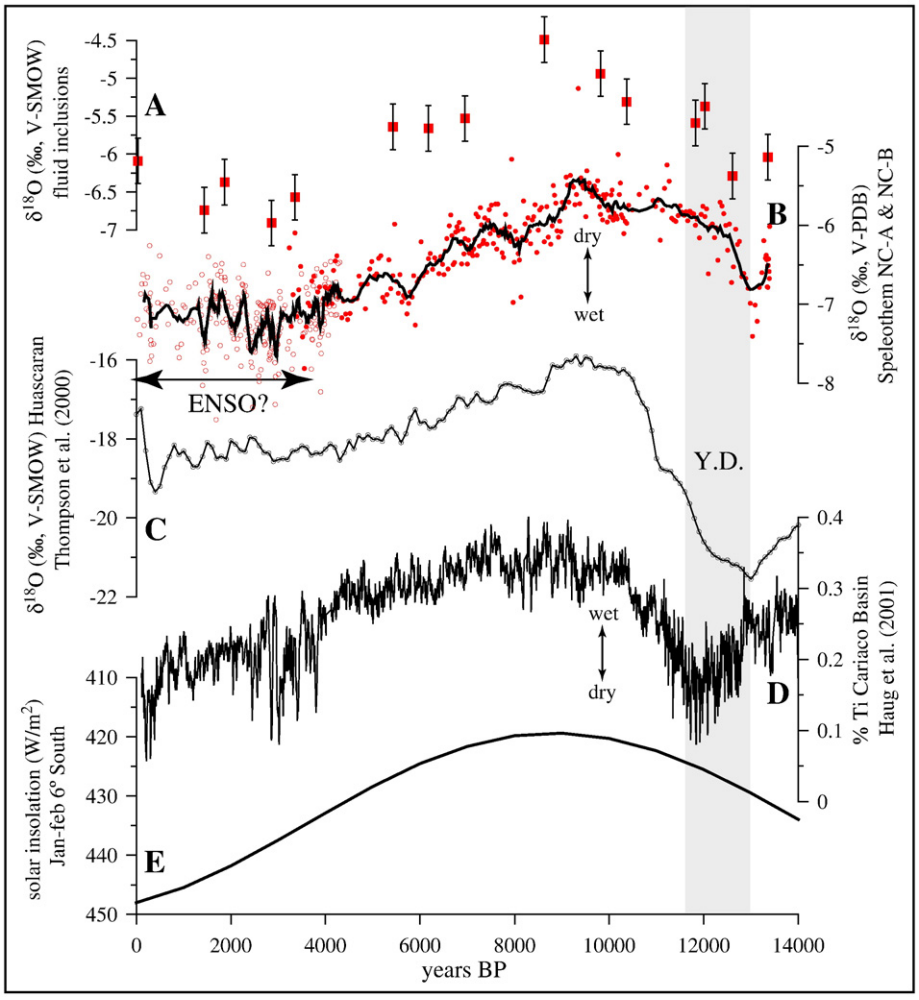

Fig. 6. Comparison of the Cueva del Tigre Perdido $\delta^{18}O$ fluid inclusion (panel A) and $\delta^{18}O$ calcite (panel B) records with the Huascaran $\delta^{18}O$ ice core record (panel C) (Thompson et al., 2000) and with the Cariaco Basin Ti% record (panel D) (Haug et al., 2001). All records show Holocene trends in phase with the solar insolation curve (panel E). Rapid climate oscillation occurs in all three records during the Younger Dryas (YD) interval (grey zone) The much stronger response in the Huascaran $\delta^{18}O$ record, compared to the Cueva del Tigre Perdido $\delta^{18}O$ record, suggests a stronger impact of YD climate change in the highlands. A comparison of the Cueva del Tigre Perdido isotope record with the Cariaco Basin Ti% record, reveals that wet YD conditions in Amazonia, coincided with Dry conditions over Northern Venezuela. This seasaw pattern suggests that climate change over Amazonia in the YD interval was primarily controlled by a general Southward movement of the ITCZ. A more detailed comparison of Cueva del Tigre Perdido calcite $\delta^{18}O$ with the Cariaco Basin Ti% record shows another similarity between the two records, in that the amplitude of high-resolution variation drastically increases in the last 4000 years. Haug et al. (2001) attributed this to increased ENSO activity from ~4000 years BP onwards.

largely controlled by the analytical uncertainty of the fluid inclusion isotope analyses (reproducibility (1σ) is <1.5‰ for δ^2H, and <0.3‰ for δ^{18}O (Vonhof et al., 2006, 2007)).

At stable Holocene temperatures, the observed 2‰ δ^{18}O variation in speleothem calcite and fluid inclusion water apparently reflects rainwater isotope variation related to increasing convective rainfall through the Holocene. Estimates of the relation between δ^{18}O and rainfall amount for the Amazon Basin, based on modern IAEA precipitation data, show that the majority of lowland IAEA stations cluster between −0.4 and −0.8‰ /100 mm (Vuille et al., 2003). For the Tigre Perdido record this would relate to a 250 to 500 mm rainfall increase from 9000 yr BP towards the present day value of ~1500 mm/yr. This must probably be taken as a maximum estimate because Cueva del Tigre Perdido is located at ~1000 m ASL, already in the foothills of the Andes, and the slope of the δ^{18}O — rainfall amount relation for highland IAEA stations is significantly steeper than for the lowlands (Vuille et al., 2003).

Tigre Perdido isotope data thus confirm that insolation-forced changes in rainfall, and not temperature, are the dominant parameter affecting the climate of lowland Amazonia, as was already suggested by several previous studies (Ramirez et al., 2003; Seltzer et al., 2000; Cruz et al., 2005).

To further investigate the transfer of atmospheric moisture from the Amazonian lowlands to the Altiplano, we compare the Tigre Perdido record with the Holocene interval of the Huascaran Ice core record (Fig. 6). There is a striking similarity in the shape of the Holocene δ^{18}O curves of both records, with a nearly constant ~12‰ offset between Huascaran and Tigre Perdido water δ^{18}O values, in good agreement with the expected orographic fractionation effect for rainfall between the two sites (Grootes et al., 1989; Rozanksi and Araguás-Araguás, 1995; Thompson et al., 2000). This suggests that the Huascaran Ice Core record accumulated from essentially the same moisture that first produced the rainfall trapped in the fluid inclusion record of Tigre Perdido. No isotope fractionation other than the orographic effect is required to match the general Holocene isotope curves between the two sites which implies little variation of the vertical atmospheric temperature gradient (lapse rate) between the two sites through the Holocene.

This situation is different for the Younger Dryas interval (Fig. 6). Here, the Ice core record shows a deep minimum in δ^{18}O values which are ~6‰ lower than those of the early Holocene (~9000 yrs BP) and ~4‰ lower than late Holocene values. The Tigre Perdido δ^{18}O record shows a much smaller Younger Dryas excursion which is ~2‰ lower than the early Holocene maximum, and comparable to modern values. The extra ~4‰ decrease of δ^{18}O values for snowfall at Huascaran compared to that of rainfall at Cueva del Tigre Perdido can be interpreted in two ways: The first option is an increased lapse rate, by which the altiplano was ~2–3°cooler in the Younger Dryas relative to the lowlands. The second option is that atmospheric circulation changes in the Younger Dryas interval drove up the mean condensation level of precipitation over the altiplano, resulting in isotopically colder snow while the lapse rate remained unchanged (Thompson et al., 2000).

The isotope signature of the Younger Dryas interval in the Tigre Perdido stalagmite suggests increased convective rainfall compared to the early Holocene interval of the same record. Isotope values are similar to modern values, suggesting rainfall amounts of ~1500 mm/yr, while the insolation was distinctly lower. Since the Younger Dryas interval typically is a higher latitude phenomenon, long distance teleconnections are required that translate high latitude cooling to the tropics. Modelling as well as proxy record studies suggest that increased meridional (North to South) sea surface temperature gradients in the Pacific and Atlantic Oceans cause convective rainfall to migrate southwards (Haug et al., 2001; Garreaud et al., 2003), leading to dryer conditions in the northern tropics (Haug et al., 2001) and wetter conditions in the southern tropics (Baker et al., 2001), where our stalagmite record is located. The seesaw pattern between the northern and southern tropical records is particularly clear in the comparison of the (southern tropics) Tigre Perdido δ^{18}O record with the (northern tropics) Cariaco basin Ti and Fe record (Haug et al., 2001; Fig. 6). Both records primarily record rainfall amounts on the South American continent over the last ~13500 years. Although thousands of kilometres apart the shape of both curves is remarkably similar, correlating dry phases in Venezuela, with wet phases in Peru (Fig. 6). The consistency of these records underlines the regional significance of the Tigre Perdido record, and again pinpoints ITCZ migration as the main control on tropical South American rainfall patterns. We tentatively suggest that even the higher-frequency variation, interpreted to be ENSO related in the interval after 3800 yrs BP in the Cariaco record (Haug et al., 2001), can be identified in the Tigre Perdido record as well (Fig. 6).

4. Conclusions

The present study shows how stalagmite fluid inclusion isotope analyses provide information on the isotope composition of paleorainfall in a datable context.

In Amazonia the δ^{18}O composition of rainwater is affected by temperature and rainfall amounts, which complicates the quantitative interpretation of fluid inclusion isotope data. However, by combination of δ^{18}O values of fluid inclusion water and its surrounding calcite, independent paleotemperatures can be calculated based on the known temperature dependency of δ^{18}O fractionation between speleothem calcite and formation water. By application of this technique to the Cueva del Tigre Perdido stalagmite record, we can distinguish between the effects of temperature and rainfall δ^{18}O values on the isotope patterns in stalagmite calcite.

Holocene climate variation, as recorded in the stalagmite, appears to be controlled by orbitally forced Southward migration of the ITCZ, causing increasing convective rainfall in our study area. While temperature remains stable, isotope variation of rainwater reflected in fluid inclusion water δ^{18}O composition suggests a ~15–30% increase in convective rainfall through the Holocene.

The isotope pattern observed in stalagmite fluid inclusions matches isotope patterns in the high Andean Huascaran Ice Core record. This similarity suggests that Andean lapse rates did not vary much through the Holocene (Vizy and Cook, 2007). Since temperatures calculated for the Cueva del Tigre Perdido stalagmite were stable, it follows that not temperature but ITCZ dynamics controlled the long trend in Holocene δ^{18}O values for Huascaran. This coupling between the two records does not exist for the Younger Dryas interval. Here, the higher amplitude δ^{18}O excursion in the Huascaran record compared to the Cueva del Tigre Perdido record, may suggests a temporarily increased lapse rate or a change in atmospheric circulation over the altiplano, forced by increased meridional sea surface temperature gradients due to cooling of higher latitudes. This same effect would account for a southward shift of the ITCZ, that caused increased rainfall in the southern tropics, and decreased rainfall in the northern tropics during the Younger Dryas.

In a wider perspective, fluid inclusion isotope analysis drastically improves paleotemperature reconstructions based on speleothem calcite δ^{18}O data, because it provides the δ^{18}O value of cave drip water through time, which is usually the most important unknown in paleotemperature equations. Results for the Cueva del Tigre Perdido show that some of the commonly used equations underestimate the actual temperatures in the cave more than others. Our poor understanding of the differences in accuracy between equations underlines the importance of further investigation into isotopic equilibrium during growth of speleothems.

In any case, the technique presented here allows for reconstruction of past rainfall δ^{18}O variation, in climate zones where ice cores are scarce or absent. This is highly significant for our understanding of

past climate variation, particularly in view of recent developments of isotope modules in climate models (Vuille et al., 2003).

Acknowledgements

We thank Quinto Quaresima and Jhon Huaman for speleological assistance and INGEMMET and INRENA for logistical support in Peru. We are indebted to Gareth Davies for U/Th dating in Amsterdam. Saskia Kars and Onno Postma gave invaluable technical assistance. This project was financially supported by NWO-WOTRO and the British Council.

Appendix A. Supplementary data

Supplementary data associated with this article can be found, in the online version, at doi:10.1016/j.epsl.2008.07.060.

References

Baker, P.A., Seltzer, G.O., Fritz, S.C., Dunbar, R.B., Grove, M.J., Tapia, P.M., Cross, S.L., Rowe, H.D., Broda, J.P., 2001. The history of south american tropical precipitation for the past 25,000 years. Science 291, 640–643.

Bar-Matthews, M., Ayalon, A., Kaufman, A., Wasserburg, G.J., 1999. The eastern Mediterranean paleoclimate as a reflection of regional events; Soreq Cave, Israel. Earth Planet. Sci. Lett. 166, 85–95.

Broecker, W.S., 1997. Mountain glaciers: Recorders of atmospheric water vapor content? Glob. Biogeochem. Cycles 11, 589–597.

Caballero, E., Jimenez De Cisneros, C., Reyes, E., 1996. A stable isotope study of cave seepage waters. Appl. Geochem 11, 583–587.

Craig, H., 1965. . The measurement of oxygen isotope palaeotemperatures. In: Tongiorgi, E. (Ed.), Stable isotopes in oceanographic studies and palaeotemperatures. Consiglio Nazionale delle Ricerche Laboratorio di Geologia Nucleare, Pisa, pp. 166–182.

Cruz, F.W., Burns, S.J., Karmann, I., Sharp, W.D., Vuille, M., Cardoso, A.O., Ferrari, J.A., Silva Dias, P.L., Viana, O., 2005. Insolation-driven changes in atmospheric circulation over the past 116,000 years in subtropical Brazil. Nature 434, 63–66.

Drysdale, R.N., Zanchetta, G., Hellstrom, J.C., Fallick, A.E., Zhao, J.X., 2005. Stalagmite evidence for the onset of the Last Interglacial in southern Europe at 129±1 ka. Geophys. Res. Lett. 32, L24708. doi:10.1029/2005GL024658.

Epstein, S., Buchsbaum, R., Lowenstam, H.A., Urey, H.C., 1953. Revised carbonate-water isotopic temperature scale. Geol. Soc. Amer. Bull. 64, 1315–1326.

Fairchild, I.J., Smith, C.L., Baker, A., Fuller, L., Spötl, C., Mattey, D., McDermott, F., E.I.M.F., 2006. Modification and preservation of environmental signals in speleothems. Earth-Science Reviews ISOtopes in PALaeoenvironmental reconstruction (ISOPAL), vol. 75, pp. 105–153.

Fleitmann, D., Burns, S.J., Mudelsee, M., Neff, U., Kramers, J., Mangini, A., Matter, A., 2003. Holocene forcing of the Indian monsoon recorded in a stalagmite from Southern Oman. Science 300, 1737–1739.

Frappier, A., Sahagian, D., Gonzalez, L.A., Carpenter, S.J., 2002. El Nino events recorded by stalagmite carbon isotopes. Science 298, 565.

Garreaud, R., Vuille, M., Clement, A.C., 2003. The climate of the Altiplano; observed current conditions and mechanisms of past changes. In: Seltzer, G.O., Rodbell, D.T., Wright, H.E. (Eds.), Late-Quaternary palaeoclimates of the southern tropical Andes and adjacent regions. Elsevier, Amsterdam, Netherlands.

Gat, J.R., Matsui, E., 1991. Atmospheric water balance in the Amazon basin: an isotopic evapotranspiration model. J. Geophys. Res. 96, 13179–13188.

Genty, D., Blamart, D., Ghaleb, B., Plagnes, V., Causse, C., Bakalowicz, M., Zouari, K., Chkir, N., Hellstrom, J., Wainer, K., Bourges, F., 2006. Timing and dynamics of the last deglaciation from European and North African d13C stalagmite profiles–comparison with Chinese and South Hemisphere stalagmites. Quat. Sci. Rev. 25, 2118–2142.

Genty, D., Blamart, D., Ouahdi, R., Gilmour, M., Baker, A., Jouzal, J., Van-Exter, S., 2003. Precise dating of Dansgaard–Oeschger climate oscillations in western Europe from stalagmite data. Nature 421, 833–837.

Grootes, P.M., Stuiver, M., Thompson, L.G., Mosley-Thompson, E., 1989. Oxygen isotope changes in tropical ice, Quelccaya, Peru. J. Geophys. Res. D, Atmospheres 94, 1187–1194.

Harmon, R.S., Schwarcz, H.P., Ford, D.C., 1978. Stable isotope geochemistry of speleothems and cave waters from the Flint Ridge-Mammoth Cave system, Kentucky: implications for terrestrial climate change during the period 230,000 to 100,000 years B.P. J. Geol. 86, 373–384.

Harmon, R.S., Schwarcz, H.P., O'Neil, J.R., 1979. D/H ratios in speleothem fluid inclusions: a guide to variations in the isotopic composition of meteoric precipitation? Earth Planet. Sci. Lett. 42, 254–266.

Haug, G.H., Haughen, K.A., Sigman, D.M., Peterson, L.C., Roehl, U., 2001. Southward migration of the Intertropical Convergence Zone through the Holocene. Science 293, 1304–1308.

Hellstrom, J., 2006. U–Th dating of speleothems with high initial 230Th using stratigraphical constraint. Quat. Geochronol. 1, 289–295.

Hellstrom, J.C., 2003. Rapid and accurate U/Th dating using parallel ion-counting multicollector ICP-MS. J. Anal. At. Spectrom. 18, 1346–1351.

Henderson, K.A., Thompson, L.G., Lin, P.N., 1999. Recording of El Niño in ice core δ^{18}O records from Nevado Huascarán, Peru. J Geophys. Res. D104, 31053–31065.

Hendy, C.H., Wilson, A.T., 1968. Palaeoclimatic data from speleothems. Nature (London) 219, 48–51.

Holmgren, K., Karlen, W., Lauritzen, S.E., Lee, T.J.A., Partridge, T.C., Piketh, S., Repinski, P., Stevenson, C., Svanered, O., Tyson, P.D., 1999. A 3000-year high-resolution stalagmite-based record of palaeoclimate for northeastern South Africa. Holocene 9, 295–309.

Hooghiemstra, H., van der Hammen, T., 1998. Neogene and Quaternary development of the neotropical rain forest: the forest refugia hypothesis, and a literature overview. Earth-Sci. Rev. 44, 147–183.

Kim, S.T., O'Neil, J.R., 1997. Equilibrium and nonequilibrium oxygen isotope effects in synthetic carbonates. Geochim. Cosmochim. Acta 61, 3461–3475.

Laskar, J., Robutel, P., Joutel, F., Gastineau, M., Correia, A.C.M., Levrard, B., 2004. A long-term numerical solution for the insolation quantities of the Earth. Astron. Astrophys. 428, 261–285.

Marengo, J.A., Nobre, C.A., 2001. General characteristics and variability of climate in the amazon basin and its links to the global climate system. In: McClain, M.E., Victoria, R.L., Richey, J.E. (Eds.), The Biogeochemistry of the Amazon Basin. Oxford University Press, pp. 17–41.

McDermott, F., Schwarcz, H.P., Rowe, P.J., 2006. Isotopes in speleothems. In: Leng, M.J. (Ed.), Isotopes in Palaeoenvironmental Research, 10. Developments in Paleoenvironmental Research. Springer, Dordrecht, the Netherlands, pp. 185–225.

Mickler, P.J., Banner, J.L., Stern, L., Asmerom, Y., Edwards, R.L., Ito, E., 2004. Stable isotope variations in modern tropical speleothems: evaluating equilibrium vs. kinetic isotope effects. Geochimica et Cosmochimica Acta 68, 4381–4393.

Ramirez, E., Hoffmann, G., Taupin, J.D., Francou, B., Ribstein, P., Caillon, N., Ferron, F.A., Landais, A., Petit, J.R., Pouyaud, B., Schotterer, U., Simoes, J.C., Stievenard, M., 2003. A new Andean deep ice core from Nevado Illimani (6350 m), Bolivia. Earth Planet. Sci. Lett. 212, 337–350.

Richards, D.A., Dorale, J.A., 2003. In: Bourdon, B., Henderson, G.M., Lundstrom, C.C., Turner, S.P. (Eds.), Uranium-series chronology and environmental applications of speleothems. Uranium-series geochemistry, vol. 52. Mineralogical Society of America and Geochemical Society, Washington, DC, United States, pp. 407–460.

Rozanksi, K., Araguás-Araguás, L., 1995. Spatial and temporal vairability of stable isotope composition of precipitation over the South American continent. Bulletin de l'Institut Français d'Études Andines 24, 379–390.

Schwarcz, H.P., Harmon, R.S., Thompson, P., Ford, D.C., 1976. Stable isotope studies of fluid inclusions in speleothems and their paleoclimatic significance. Geochim. Cosmochim. Acta 40, 657–665.

Schwarcz, H.P., Yonge, C.J., 1983. In Paleoclimates and Paleowaters: A Collection of Environmental Isotope Studies. IAEA, Vienna, p. 115.

Seltzer, G., Rodbell, D., Burns, S., 2000. Isotopic evidence for Late Quaternary climatic change in tropical South America. Geology 28, 35–38.

Shackleton, N.J., Opdyke, N.D., 1973. Oxygen isotope and palaeomagnetic stratigraphy of Equatorial Pacific core V28-238: oxygen isotope temperatures and ice volumes on a 105 year and 106 year scale. Quat. Res. 3, 39–55.

Thompson, L.G., Mosley-Thompson, E., Davis, M.E., Lin, P.N., Henderson, K.A., Cole, D.J., Bolzan, J.F., Liu, K.B., 1995. Late Glacial Stage and Holocene tropical ice core records from Huscaran, Peru. Science 269, 46–50.

Thompson, L.G., Mosley-Thompson, E., Henderson, K.A., 2000. Ice-core palaeoclimate records in tropical South America since the Last Glacial Maximum. J. Quat. Sci. 15, 377–394.

Thompson, L.G., Mosley-Thompson, E., Brecher, H., Davis, M.E., León, B., Les, D., Lin, P.N., Mashiotta, T., Mountain, K., 2006. Abrupt tropical climate change: past and present. PNAS 103, 10536–10543.

Vacco, D.A., Clark, P.U., Mix, A.C., Cheng, H., Edwards, R.L., 2005. A speleothem record of Younger Dryas cooling, Klamath Mountains, Oregon, USA. Quat. Res. 64, 249–256.

Vimeux, F., Gallaire, R., Bony, S., Hoffmann, G., Chiang, J.C.H., 2005. What are the climate controls on [delta]D in precipitation in the Zongo Valley (Bolivia)? Implications for the Illimani ice core interpretation. Earth Planet. Sci. Lett. 240, 205–220.

Vizy, E.K., Cook, K.H., 2007. Relationship between Amazon and high Andes rainfall. J. Geophys. Res. 112. doi:10.1029/2006JD007980.

Vonhof, H.B., Atkinson, T.C., van Breukelen, M.R., Postma, O., 2007. Fluid inclusion hydrogen and oxygen isotope analyses using the "Amsterdam Device": a progress report. Geophys. Res. Abstr 9, 05702.

Vonhof, H.B., van Breukelen, M.R., Postma, O., Rowe, P.J., Atkinson, T.C., Kroon, D., 2006. A continuous-flow crushing device for on-line d2H analysis of fluid inclusion water in speleothems. Rapid Commun. Mass Spectrom. 20, 2553–2558.

Vuille, M., Bradley, R.S., Werner, M., Healy, R., Keimig, F., 2003. Modeling δ^{18}O in precipitation over the tropical Americas; 1. Interannual variability and climatic controls. J. Geophys. Res. 8, 4174.

Wang, Y.J., Cheng, H., Edwards, R.L., An, Z.S., Wu, J.Y., Shen, C.C., Dorale, J.A., 2001. A high-resolution absolute-dated late Pleistocene monsoon record from Hulu Cave, China. Science 294, 2345–2348.

Wang, Y., Cheng, H., Edwards, R.L., He, Y., Kong, X., An, Z., Wu, J., Kelly, M.J., Dykoski, C.A., Li, X., 2005. The Holocene Asian Monsoon: links to solar changes and North Atlantic Climate. Science 308, 854–857.

Yuan, D., Cheng, H., Edwards, R.L., Dykoski, C.A., Kelly, M.J., Zhang, M., Qing, J., Lin, Y., Wang, Y., Wu, J., Dorale, J.A., An, Z., Cai, Y., 2004. Timing, duration, and transitions of the last Interglacial Asian Monsoon. Science 304, 575–578.